Catena 137 (2016) 237–243

Contents lists available at ScienceDirect

Catena

journal homepage: www.elsevier.com/locate/catena

Evaluation of kinetic energy and erosivity potential of simulated rainfall using Laser Precipitation Monitor

Derege Tsegaye Meshesha [a,*], Atsushi Tsunekawa [b], Mitsuru Tsubo [c], Nigussie Haregeweyn [b,d], Firew Tegegne [a,b]

[a] Institute of Disaster Risk Management and Food Security Studies, Bahir dar University, Ethiopia
[b] Arid Land Research Centre, Tottori University, 1390 Hamasaka, Tottori 680-0001, Japan
[c] Institute for Soil, Climate and Water, Agricultural Research Council, 600 Belvedere Street, Arcadia, Pretoria 0083, South Africa
[d] Department of Land Resources Management and Environmental Protection, Mekelle University, Tigray P.O. Box 231, Ethiopia

ARTICLE INFO

Article history:
Received 25 December 2014
Received in revised form 10 August 2015
Accepted 27 September 2015
Available online 22 October 2015

Keywords:
Arid region
Raindrop size distribution
Kinetic energy
Erosivity
Rainfall simulator
Laser Precipitation Monitor

ABSTRACT

Rainfall kinetic energy is a widely recognized indicator of a raindrop's ability to detach soil particles in rainsplash erosion. However, it is challenging to estimate the kinetic energy (KE) of a given rain event, because it involves analysis of the terminal velocity and drop size distribution (DSD) of raindrops. A preferred alternative is to relate KE to rainfall intensity. Therefore we sought to characterize simulated rainfall, establish a relationship between kinetic energy and intensity as a function of both time (KE_t, J m^{-2} h^{-1}) and volume (KE_{vol}, J m^{-2} mm^{-1}), and examine the erosivity potential of each event. A rainfall simulator and Laser Precipitation Monitor (optical disdrometer) were used to characterize raindrop size, terminal velocity and KE at different rainfall intensities (1.5 to 202 mm h^{-1}). Values of KE_t ranged from 26.67 to 5955 J m^{-2} h^{-1} and KE_{vol} ranged from 16.10 to 34.85 J m^{-2} mm^{-1}, which is comparable to values determined from natural rain of similar intensity ranges. A power-law function and a polynomial function between KE_t and rainfall intensity had coefficients of determination (R^2) of 0.99 and 0.98 ($P < 0.0001$), respectively. The best-fitting relationship between KE_{vol} and intensity was a power-law function ($R^2 = 0.95$; $P < 0.001$). We found that erosivity had a very strong correlation with rainfall depth ($R^2 = 0.99$; $P < 0.0001$) in power-law function. Furthermore, regardless of rainfall intensity, KE is more strongly correlated with raindrop size than volume of raindrop.

1. Introduction

Soil erosion by water is a two-phase process that consists of detachment of soil particles from the soil mass by rainsplash and transportation of detached particles by running water or runoff (Morgan, 2005). Rainsplash erosion is caused by the kinetic energy of raindrops that strike the soil and throw particles into the air (Sempere-Torres et al., 1992; Wischmeier and Smith, 1978). Running water is a more powerful erosive agent than rainsplash because raindrops use most of their energy in detachment and thus have less energy for transport than overland flow (Gilley and Finkner, 1985; Grismer et al., 2008; Kinnell, 1990). Information about the drop size distribution (DSD) of raindrops is fundamental for efforts to predict soil erosion and develop mitigation strategies, because raindrop properties govern rainfall erosivity through the kinetic energy of drops (Blanchard, 1953; Lu et al., 2008).

The available energy for erosion is analyzed in terms of potential and kinetic energy (Morgan, 2005). Potential energy (*PE*) is computed as the product of raindrop mass (m), the raindrop's height above the ground (h) and the acceleration of gravity (g). The potential energy is converted into the kinetic energy (*KE*) of raindrop motion, which is related to the mass and terminal velocity (V_t) of the drop (Kinnell, 1990; Salles et al., 2002; Van Dijk et al., 2002). The total kinetic energy of a rainfall event is calculated by summing the individual kinetic energies of raindrops with the aid of information on DSD and raindrop terminal velocity (Sharma et al., 1995).

The basic expression of erosivity is based on the kinetic energy of the rain and its maximum 30-min intensity (Wischmeier and Smith, 1978). Kinetic energy is relatively more difficult to determine because measurement of DSD is cumbersome, varies with different storm types and requires a continuous record of the rainfall event. Even when DSD information has been collected, the other necessary data (e.g. terminal velocity) are seldom available and are not among commonly collected metrological parameters. Therefore, researchers often estimate KE empirically from its relationship to rainfall intensity (Hudson, 1965; Lal, 1998; Meshesha et al., 2013; Nyssen et al., 2005; Onaga et al., 1988). However, because this relationship varies with sample size, methods and rainfall types, it is not considered reliable at all localities (Van Dijk et al., 2002). For example, cyclonic rain in the temperate zone is mainly composed of small and average size raindrops whereas high-intensity tropical thunderstorms have a greater proportion of large drops. Thus, the rain energy of the two storm types differs even at the same

* Corresponding author.
E-mail address: deremesh@yahoo.com (D.T. Meshesha).

http://dx.doi.org/10.1016/j.catena.2015.09.017
0341-8162/

rainfall intensity (McIsaac, 1990; Meshesha et al., 2013). Therefore, in this study, we investigated the kinetic energy and erosivity of rainstorms using simulated rainfall.

The main objective of this study was to analyze the DSD, kinetic energy and erosivity of different events, using data collected from a rainfall simulator and an optical disdrometer. We also sought to establish an alternative relationship between intensity and kinetic energy, and evaluate the erosivity potential of different events.

2. Materials and methods

2.1. Rainfall simulator

Erosivity indexes can be developed using natural or simulated rain. One advantage of rainfall simulation is its ability to emulate natural rainfall in a controlled manner, and DSD can be adjusted to a degree. By controlling rainfall properties such as duration, intensity, rainfall depth and fluctuation in intensity, simulated rain helps to eliminate the erratic and unpredictable variability of natural rain.

We used a drop-forming type of rain simulator at the Arid Land Research Centre of Tottori University, Japan, that consists of a computer control system, water reservoir and pump, oscillating screen and hypodermic tubes that distribute the water. Its height of 12 m is in principle sufficient for raindrops >3 mm to achieve their terminal velocity (Fig. 1a). More detailed descriptions of the simulator are given by Abd Elbasit et al. (2010).

At first, the rainfall simulator had to be calibrated so as to get the intensity of different flow rates. Thus, the water from the available tanks (3 in number) was pumped at different flow rates and the corresponding intensity was measured and recorded, thereby, a total of 20 different intensities were simulated (1.5–202 mm/h) for corresponding flow rates (19.5–500 l/h). All the raindrops from the beginning to the end of the events were included in the calculation of average intensity, depth and characterization of the drop size distributions.

2.2. Laser Precipitation Monitor (LPM)

There are several techniques to measure the DSD of rainfall. Manual methods are tedious, time consuming, of limited accuracy and inadequate when raindrops fall in large numbers and at changeable rates (Meshesha et al., 2014). Automatic sampling devices that produce continuous records of DSD and raindrop counts include acoustic (piezoelectric transducers), electromechanical and optical disdrometers.

The Laser Precipitation Monitor (LPM), an optical disdrometer (Adolf Thies GmbH & Co. KG, Germany), was used in this study (Fig. 1b and c). Precipitation particles falling through an infrared laser beam (780 nm) in a sensor with a 45 cm^2 cross section are characterized in terms of their diameter and velocity by processing the signal of a photodiode that receives the beam (Fig. 1c). The device classifies drops by diameter from 0.16 mm to ~9 mm and determines their terminal velocity, then its software (version 1.04 07/2003) groups the raindrops into different classes of drop size. Using the assumption that raindrops are spherical, the diameter is used to calculate the mass and velocity of raindrops and derive their corresponding kinetic energy.

To avoid backsplash effect of raindrops, the sensor was positioned 1 m above the ground and thus the actual distance between the sensor area and the dripper (simulator) was 11 m. Furthermore, the sensor was installed parallel to the ground and perpendicular (90°) to the mast (as suggested by the company).

2.3. Kinetic energy expressions

A favored expression of rainfall erosivity is an index based on the kinetic energy of the rain (Renard et al., 1991; Wischmeier and Smith, 1978). Rainfall kinetic energy can be obtained from direct measurements, such as by force transducers or acoustic devices (Abd Elbasit et al., 2010; Jayawardena and Rezaur, 2000), or by calculation from the measured DSD and terminal velocity of raindrops using a disdrometer.

Kinetic energy is expressed in two forms in rainfall data analyses: kinetic energy per unit area per unit time (KE_t, J m^{-2} h^{-1}) and kinetic

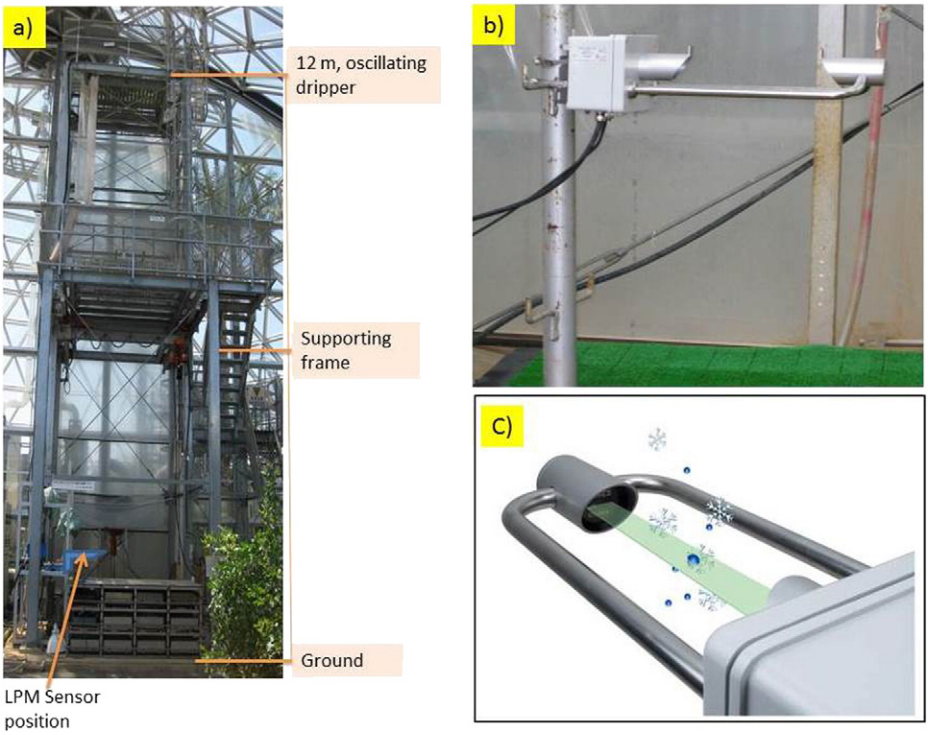

Fig. 1. Photographs of the rainfall simulator (a) and LPM sensor (b; location shown in a), and diagram showing the measuring principle of the LPM (c).

energy content, which is a function of rainfall depth (KE_{vol}, J m^{-2} mm^{-1}). Because drop size is strongly related to terminal velocity and kinetic energy, KE of a given drop is derived from the product of its mass and the square of its terminal velocity.

The instrument used in this study sums the number of drops in each drop-size class along with their falling velocity and produces the output for every 1 min time period. We aggregated these 1-min measurements into energy of total rainfall using the following expression:

$$KE_t = \left(\frac{\rho\pi}{12}\right)\left(\frac{1}{10^6}\right)\left(\frac{3600}{t}\right)\left(\frac{10^4}{A}\right)\sum_{i=1}^{n} N_i D_i^3 \quad v_{Di}^2, \tag{1}$$

where ρ is the density of water (kg m^{-3}), t is the exposure time (s), N_i is the number of drops in class i, D_i is the drop diameter of class i (mm), v^2_{Di} is the falling velocity of D_i (m s^{-1}) and A is the sampling area of the sensor (45 cm^2). Similarly, KE_{vol} was derived from the following equation:

$$KE_{vol} = \left(\frac{\rho\pi}{12}\right)\left(\frac{1}{10^6}\right)\left(\frac{1}{vol}\right)\left(\frac{10^4}{A}\right)\sum_{i=1}^{n} N_i D_i^3 \quad v_{Di}^2, \tag{2}$$

where *vol* is the total depth of the rainfall event.

2.4. Rainfall erosivity indexes

The rainfall erosivity factor R (MJ mm ha^{-1} h^{-1}) evaluates the capacity of rain to erode unprotected soil. Renard and Freimund (1994) summarized previously published estimates of R for various parts of the world. Wischmeier and Smith (1958) found that soil loss by rainsplash, sheet and rill erosion is related to the product of rainfall kinetic energy E and maximum 30-min rainfall intensity I_{30}, or EI_{30}. Monthly R values are obtained from the sum of EI_{30} values of all rainfall events within a month, and similarly annual R values are the sum of the EI_{30} values of storms in a year.

There has been concern over the validity of the EI_{30} index for the high-intensity rains of tropical regions and higher altitudes, and also for rains over the ocean where raindrops and their energies are small. There is no clear justification that I_{30} is the optimum value for this parameter. Moreover, this index assumes that erosion occurs even at light rain intensity, whereas Hudson (1965) argued that erosion requires a rain intensity greater than 25 mm h^{-1} and based on this assumption he developed a simpler alternative index, but Stocking and Elwell (1973) concluded that EI_{30} is the better index. Thus, it remains the most widely accepted index for erosivity estimates in the process-based approach.

The other commonly used index of rainfall erosivity is the Fournier Index (FI), which is the ratio p^2/P, where p is the wettest monthly precipitation and P is the mean annual precipitation, or the Modified Fournier Index (MFI), which is the ratio of the squared monthly rainfalls in a year over the total annual rainfall (Meshesha et al., 2014; Oduro-Afriyie, 1996). Both of these indexes yield rough estimates of rainfall intensity and erosivity because they are based on monthly and annual rainfall without any consideration of raindrop sizes and the energy of individual storms. Carolina et al. (2008) and Meshesha et al. (2014) used MFI to estimate the temporal variation and spatial distribution of rainfall erosivity and assess its implication for long-term soil erosion in Uruguay and Ethiopia, respectively.

In this study, we calculated erosivity from rainfall kinetic energy and maximum 30-min intensity, and established a linear relationship with rainfall depth.

3. Results and discussion

3.1. Drop size distribution and kinetic energy of simulated rainfall

For each of 20 combinations of flow rate and rainfall intensity, we operated the rainfall simulator for 25 to 40 min to get optimum results for DSD and corresponding kinetic energy (Table 1). The simulated rain varied from 0.69 to 99.2 mm in depth and from 1.5 to 202 mm h^{-1} in intensity. Data for 4,189,814 drops were recorded. All raindrops from the beginning to the end of a given event were used to calculate average intensity, energy, depth and to characterize DSD.

Values of KE_{vol} ranged from 16.10 to 34.85 J m^{-2} mm^{-1} while KE_t ranged from 26.67 to 5955.51 J m^{-2} h^{-1}. Van Dijk et al. (2002) analyzed measurements from around the world and found that when the data were of high quality, KE_{vol} ranged from 11 to 36 J m^{-2} mm^{-1} with average maximum values of about 29 J m^{-2} mm^{-1} and average minimum values of about 12 J m^{-2} mm^{-1}. Our observations were generally within that range, except that the minimum value was slightly higher than the stated range. Van Dijk et al. (2002) also reported that for the intensity range between 40 and 100 mm h^{-1}, the average KE_{vol} obtained was between 23 and 28 J m^{-2} mm^{-1}. The median volume drop diameter (D_{50}) ranged between 1.94 and 7.25 mm and was relatively large with

Table 1
DSD and kinetic energy of simulated rainfall for different intensities.

No.	Flow rate (l/h)	Intensity (mm h^{-1})	Rain depth (mm)	Total drops	Max. drops/min	CV (%)	D_{50} (mm)	KE_{vol} (J m^{-2} mm^{-1})	KE_t (J m^{-2} h^{-1})
1	19.5	1.5	0.69	5472	272	98.6	1.94	16.10	26.67
2	41.8	4.2	1.75	12,213	577	114.2	2.23	18.92	85.33
3	73.9	8.4	3.4	40,365	2418	92.3	2.26	20.11	151.25
4	100.9	12.8	6.17	60,420	2750	95.1	2.27	19.63	261.59
5	124.2	16.7	10.3	67,904	3851	92.4	2.76	22.41	353.56
6	150.5	21.6	7.9	60,734	4976	151.3	3.72	22.04	472.73
7	176.4	27.1	13.5	187,004	7861	52.2	4.26	24.79	553.70
8	204.2	34.2	23.4	365,839	11,187	73.6	3.25	27.69	678.99
9	228.6	49.3	19.6	234,588	14,701	68.6	3.85	27.43	1062.14
10	250.1	56.9	25.6	538,437	29,359	55.8	4.25	27.66	1165.32
11	275.8	60.6	34.4	363,977	17,462	88.8	3.82	29.26	1277.18
12	301.9	66.2	25.4	279,956	18,343	99.8	3.26	28.58	1109.21
13	328.5	71.8	27.5	326,465	23,417	62.7	4.65	28.40	1246.38
14	354.4	74.9	43.7	172,011	7749	57.9	6.25	31.15	2310.19
15	379.6	80.4	40.2	289,373	18,310	76.6	5.25	31.66	1855.11
16	404.9	95.8	51.1	196,976	7505	96.2	5.26	33.85	2252.06
17	429.5	107.7	50.7	311,997	14,442	80.6	5.26	32.11	2723.81
18	456.8	128.6	72.9	204,077	7469	150.0	7.26	34.13	3656.13
19	480.9	156.9	65.4	190,961	14,360	82.6	7.26	31.73	4741.38
20	500	202	99.2	281,045	15,874	82.5	7.25	34.85	5955.51

Where, CV (coefficient of variation); *D*50 (median volume drop diameter); KEvol (kinetic energy content); KEt (Kinetic energy time).

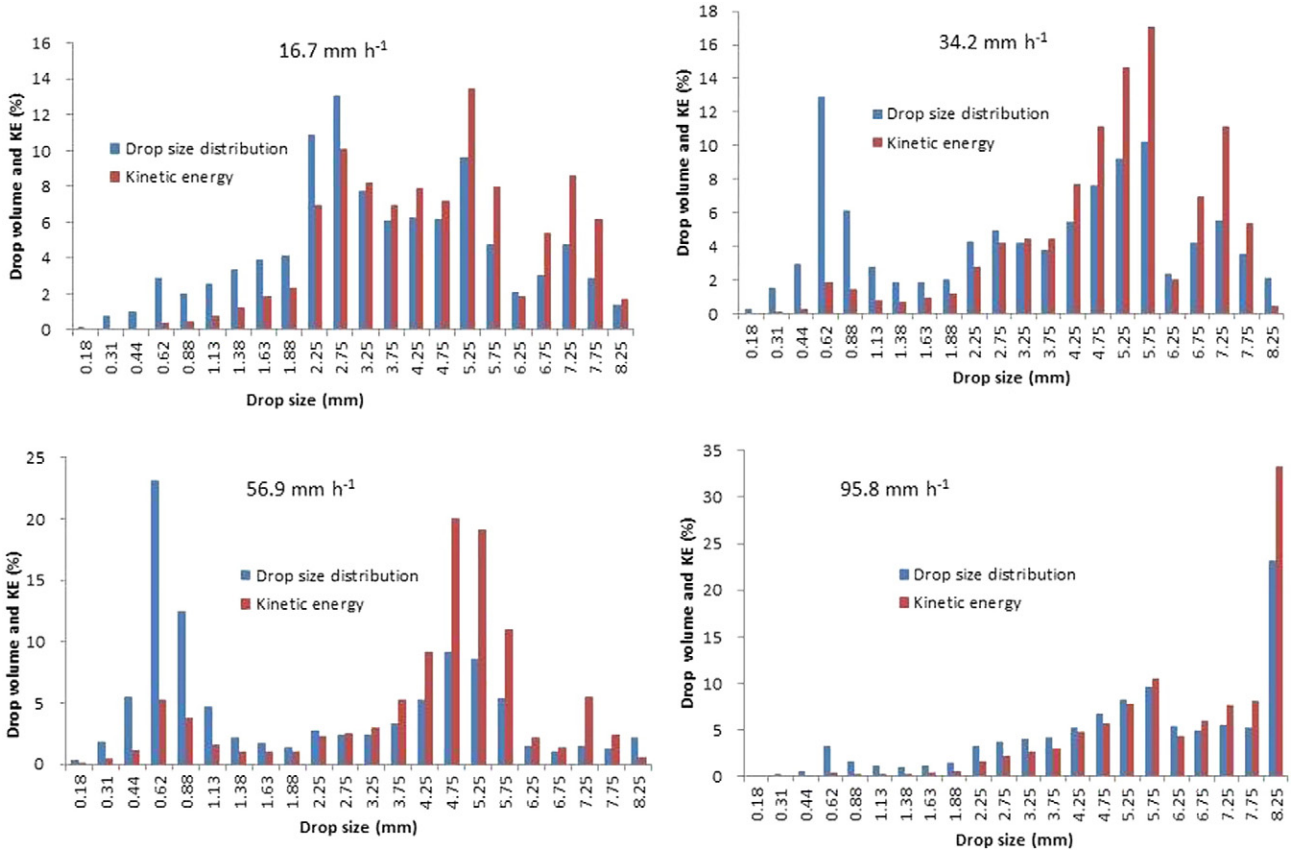

Fig. 2. Relationship between simulated rainfall drop volume and kinetic energy at different intensities.

respect to natural rain (Table 1) of commensurate intensity. In natural rain, D_{50} increases with intensity to a certain level above which it starts decreasing as turbulence makes larger drop sizes unstable, whereas that is not the case in simulated rain. The coefficient of variation (CV) was high and variable at different intensities (55.8% to 151.3%), which means that for a given rainfall event, regardless of its intensity, the drop sizes were highly diverse. We found no consistent relationship between intensity and CV, and some rainfall events had a CV exceeding 1 (or 100%), implying that the standard deviation of drop sizes was greater than the mean drop size.

Our observations indicated that KE_{vol} is more strongly correlated with raindrop size than raindrop volume, regardless of rainfall intensity (Fig. 2). Thus the total KE_{vol} of rainfall is highly dependent on DSD. For example, in simulations with intensities of 16.7, 34.2, 56.9 and 95.8 mm h^{-1}, drops smaller than 2.75 mm accounted for 45%, 42%, 58% and 17% of the total raindrop volume but generated only 24%, 19%, 20%, and 6% of the total storm energy, respectively. On the other hand, drops larger than 5.25 mm made up 28%, 37%, 21%, and 62% of drop volume and contributed 37%, 57%, 42%, and 77% of the total KE_{vol}, respectively. Hence, even though smaller raindrop sizes contribute more volume, they have lower cumulative energy due to their smaller mass, while relatively few large drops generate cumulative energy out of proportion to their volume.

Our results conflict with the conclusion of Abd Elbasit et al. (2010) that "drop volume (%) and KE (%) showed good agreement." However, their observations excluded drops smaller than 1 mm and larger than

Table 2
Relationships between KE_{vol} (J m^{-2} mm^{-1}) and intensities (mm h^{-1}) in previous studies.

Equation	Region	Reference
$KE = 11.87 + 8.73 \log I$	Washington DC, USA	Wischmeier and Smith (1978)
$KE = 29.8–127.5\ I^{-1}$	Zimbabwe	Hudson (1965)
$KE = 8.95 + 8.44 \log I$	Ottawa, Canada	Marshall and Palmer (1948)
$KE = 6.261 \ln I + 9.771$	Denmark	Pedersen and Hasholt (1995)
$KE = 9.81 + 11.25 \log I$	Central Italy	Zanchi and Torri (1980)
$KE = 9.81 + 10.6 \log I$	Okinawa, Japan	Onaga et al. (1988)
$KE = 35.9\ [1–0.56\ \exp.(-0.034I)]$	Portugal	Coutinho and Tomás (1995)
$KE = 29\ [1–0.6\ \exp.(-0.04I)]$	Australia	Rosewell (1986)
$KE = 36.8\ [1–0.69\ \exp.(-0.038I)]$	Hong Kong, China	Jayawardena and Rezaur (2000)
$KE = 38.4\ [1–0.54\ \exp.(-0.029I)]$	Barcelona, Spain	Cerro et al. (1998)
$KE = 28.3\ [1–0.52\ \exp.(-0.042I)]$	Universal relation	Van Dijk et al. (2002)
$KE = 36.65\ (1 - (0.6/I))$	Northern Ethiopia	Nyssen et al. (2005)
$KE = 7.56 \ln (I) + 9.98$	Central Rift Valley, Ethiopia	Meshesha et al. (2013)
$KE = 14.18\ I^{0.172}$	Simulated rainfall, Japan	Present study (2015)

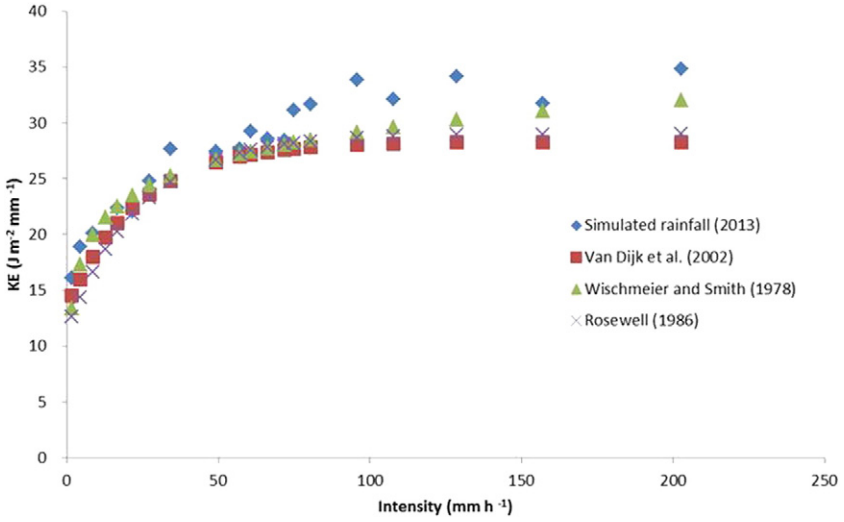

Fig. 3. Comparison of established relationship between KE_{vol} and rainfall intensity in simulated and natural rainfall.

5 mm. Our results are in agreement with the conclusion of Clarke and Walsh (2007), who used a similar rainfall simulator and found that <1 mm drops (61%) generated only ~1% of the total KE_{vol} and 1–5 mm drops (38%) generated 75% of the total KE_{vol}. Therefore, in general, our finding supports the fact that KE_{vol} is influenced more by drop size than by drop volume.

3.2. Relationship between KE_{vol} and intensity

Of various empirical relationships proposed between kinetic energy content (KE_{vol}) and rainfall intensity (I), the most widely used are log-based and exponential functions (Table 2). Such relationships are essential for deriving kinetic energy from rainfall intensity. However, they differ substantially in their D_{50} values for rains of the same intensity but of different types or in different regions.

Van Dijk et al. (2002) noted that the variation in these equations arises mainly from variations in measurement techniques, rainfall types, sample sizes or biases and methods of interpretation. Grismer (2011) proposed a new general equation, but found that it made overpredictions in areas with strong coastal influence and underpredictions in semi-arid and sub-humid places.

We used our simulated rainfall data from 20 events to establish the following power-based and logarithm-based relations between KE_{vol} and intensity:

$$KE_{vol} = 14.18\, I^{0.172} \left(R^2 = 0.95; P<0.001\right) \quad (3)$$

$$KE_{vol} = 4.24 \ln(I) + 11.68 \left(R^2 = 0.92; P<0.001\right). \quad (4)$$

Both equations have fairly high correlation coefficients, but the power-law function of Eq. (3) provides the better fit to the data, and we compared it to other equations derived from natural rain in Fig. 3. Unsurprisingly, for any given intensity the corresponding KE_{vol} was higher in our experiments than in natural rain because drop sizes are larger in simulated rain. This result was also supported by the D_{50} analysis in Section 3.1.

Our results also show that there are strong fluctuations in energy with time. The variation increased with intensity, ranging from 5.7 to 29.1, 12.6 to 33.2 and 9.14 to 43.4 J m^{-2} mm^{-1} for intensities of 8.4, 21.6 and 74.9 mm h^{-1}, respectively (Fig. 4). This implies that, for a given intensity, the erosive power of rainfall varies widely during a rainfall event.

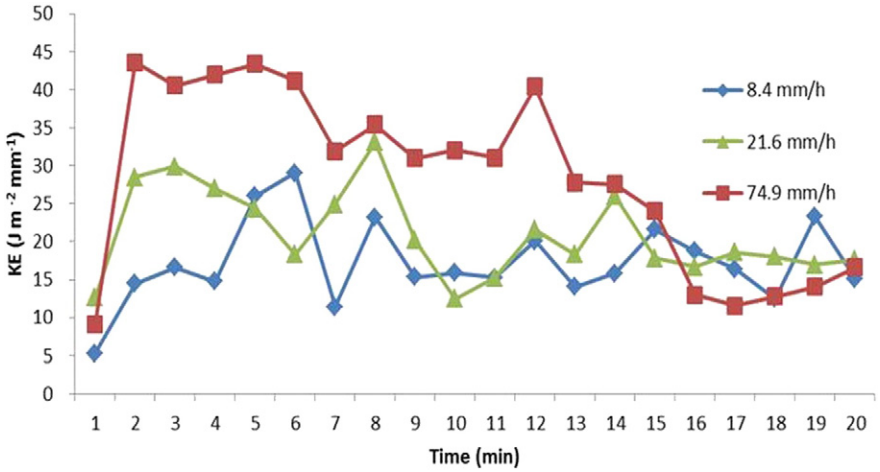

Fig. 4. Fluctuation of KE_{vol} in different 1-min time intervals at three different rainfall intensities.

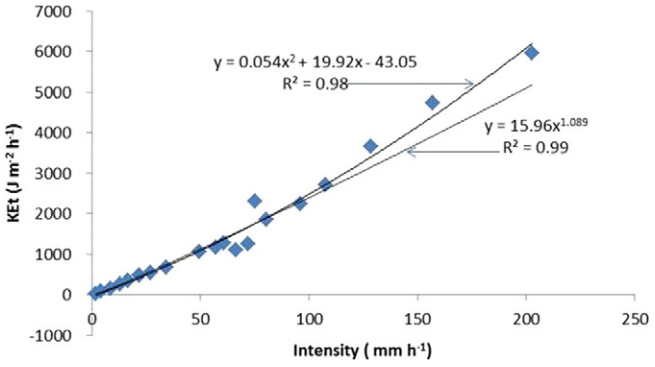

Fig. 5. Scatter plot of KE_t versus I data with power-law and polynomial functions.

3.3. Relationship between KE_t and intensity

We used simulated rains with intensities of 1.5 to 202 mm h^{-1} to analyze kinetic energy as a function of time (KE_t), and obtained results between 26.67 and 5995.51 J m^{-2} h^{-1}. In natural rainfall events, KE_t ranges from 200 to ~3000 J m^{-2} h^{-1} for intensities between 1 and 42 mm h^{-1}, but it can reach up to 6000 J m^{-2} h^{-1} for short and high-intensity rainfall events (Grismer, 2011; Morgan, 2005; Van Dijk et al., 2002). The maximum KE_t in our simulated rain, obtained at the highest intensity, was close to the record 6000 J m^{-2} h^{-1} documented by Madden et al. (1998) in natural rain. We observed KE_t values much smaller than the lower threshold of natural rainfall, but our results for the average and upper limit values were closer to those for natural rainfall. We generated the following polynomial and power-law functions relating KE_t and intensity, both of which yielded excellent fits to the data (Fig. 5):

$$KE_t = 0.054I^2 + 19.92I - 43.05\left(R^2 = 0.98; P<0.0001\right), \quad (5)$$

$$KE_t = 15.96I^{1.09}\left(R^2 = 0.99\right). \quad (6)$$

Although these yield a better fit, in most cases a function relating KE_{vol} and I is used because rainfall depth data are more accurate and accessible from local metrological stations than rainfall duration data, which are subject to bias and errors.

3.4. Evaluating erosivity values of simulated rainfall

Table 3 summarizes the erosivity values (EI_{30}) of our 20 experimental rainfall events, which ranged from 0.16 to 5896.98 MJ mm ha^{-1} h^{-1}. The result indicated that EI_{30} values were strongly correlated with rainfall depth (Fig. 6). Hudson (1971) found no clear relationship between EI_{30} and rainfall depth; however, Garollina et al. (2007) showed that it is arithmetically possible to express EI_{30} in terms of the rainfall depth. The very high coefficient of determination between rainfall depth and erosivity ($R^2 = 0.99$; $P < 0.0001$) suggests that nearly 99% of the variation in erosivity is accounted for by rainfall depth.

The relationship between rainfall erosivity R and depth D is expressed by the following power-law equation:

$$R = 0.366D^{2.064}\left(R^2 = 0.99\right). \quad (7)$$

The relationship is highly stronger as compared to the finding of Hassan (2011) for natural rainfall in Iraq, in which the value of R^2 was about 0.83. However, this model based on our simulated rain data should be applied to natural rain with great caution because the rainfall depth (e.g. rainfall duration) was controlled more strictly than is probably the case in natural rain at the same intensity. Other researchers have established such relationships in natural rainfall and found weaker correlations than reported in our study. For example, Roose (1975) showed that annual rainfall erosivity in Ivory Coast and Burkina Faso could be estimated from annual rainfall depth (mm) and multiplication of 0.5. In general, a relationship between rainfall erosivity and depth should take into account the character of local rainfall, not only rainfall depth but also the local rainfall intensity, drop size and energy.

4. Conclusion

We used a rainfall simulator and LPM to analyze DSD, D_{50}, kinetic energy and erosivity potential of rainfall intensities ranging from 1.5 to 202 mm h^{-1}. For all rainfall intensities, the corresponding KE_{vol} was higher than for natural rain as simulated rain has larger drop sizes. This finding indicates that the kinetic energy of rainfall was more

Table 3
Erosivity values of different rainfall intensities and depths.

No.	Average intensity (mm h^{-1})	Rain depth (mm)	Duration (min)	Maximum intensities (mm h^{-1})				Absolute KE (J)	Energy per area (J m^{-2})	Erosivity (MJ mm ha^{-1} h^{-1})
				1 min	5 min	15 min	30 min			
1	1.5	0.69	25	3.4	1.6	1.5	1.4	0.05	11.11	0.16
2	4.2	1.75	25	7.34	4.2	3.7	3.5	0.16	35.56	1.35
3	8.4	3.4	24	11.5	8.8	8.3	8.6	0.27	60.50	5.20
4	12.8	6.17	29	21.6	12.24	12.4	11.6	0.57	126.44	14.67
5	16.7	10.3	37	47.3	34.1	23.4	17.02	0.98	218.03	37.11
6	21.6	7.9	22	40.3	29.8	25.8	25.8	0.78	173.33	44.72
7	27.1	13.5	30	34.8	28.7	28.3	26.9	1.25	276.85	74.47
8	34.2	23.4	41	61.2	42.8	40.5	38.9	2.09	463.97	180.49
9	49.3	19.6	24	76.2	58.8	56.1	46.1	1.91	424.86	195.86
10	56.9	25.6	27	87.6	69.4	64.8	54.9	1.06	236.48	129.83
11	60.6	34.4	34	118.2	93.6	76.4	65.7	3.26	723.74	475.50
12	66.2	25.4	23	95.7	85.2	67.6	63.5	1.91	425.20	270.00
13	71.8	27.5	23	98.9	82.8	80.4	69.9	2.15	477.78	333.97
14	74.9	43.7	35	185.4	117.6	99.2	74.7	6.06	1347.61	1006.67
15	80.4	40.2	30	165.8	135.1	113.6	78.7	4.17	927.55	729.99
16	95.8	51.1	32	188.2	154.4	99.2	95.01	5.40	1201.10	1141.16
17	107.7	50.7	28	187.2	150.3	129.6	105.8	5.72	1271.11	1344.84
18	128.6	72.9	34	273.4	234.1	140.8	135.8	9.32	2071.81	2813.52
19	156.9	65.4	25	304.9	208.8	156.9	156.2	8.89	1975.57	3085.85
20	202	99.2	28	394.9	373.2	223.6	212.18	12.51	2779.24	5896.98

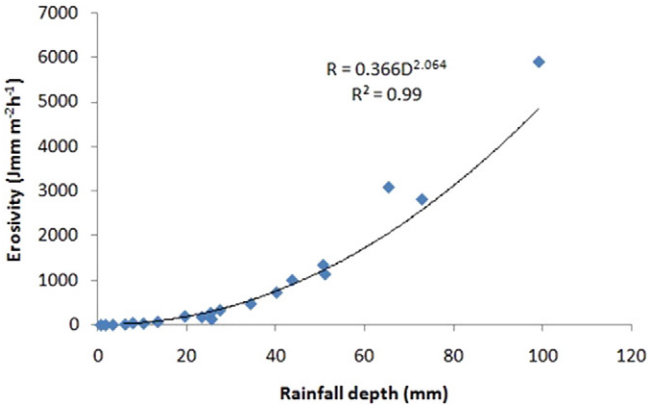

Fig. 6. Relationship between rainfall erosivity (EI_{30}) and rainfall depth.

strongly correlated with drop size than drop volume, regardless of rainfall intensity. A power-law function relating KE_{vol} and intensity yielded the best fit to observations ($R^2 = 0.95$; $P < 0.001$), and both polynomial and power-law functions yielded excellent fits to the relationship between KE_t and intensity ($R^2 = 0.98$ and 0.99 ($P < 0.0001$), respectively).

The relationship between rainfall depth and erosivity (EI_{30}) had a very high coefficient of determination ($R^2 = 0.99$). However, this equation should be applied to natural rain with caution because rainfall duration was tightly controlled in our simulations.

References

Abd Elbasit, M.A.M., Yasuda, H., Salmi, A., Anyoji, H., 2010. Characterization of rainfall generated by dripper-type rainfall simulator using piezoelectric transducers and its impact on splash soil erosion. Earth Surf. Process. Landf. 35, 466–475.

Blanchard, D.C., 1953. Raindrop size distribution in Hawaiian rains. J. Meteorol. 10, 457–473.

Cerro, C., Bech, J., Codina, B., Lorente, J., 1998. Modeling rain erosivity using disdrometric techniques. Soil Sci. Soc. Am. J. 62, 731–735.

Clarke, M.A., Walsh, R.P.D., 2007. A portable rainfall simulator for field assessment of splash and Slope wash in remote locations. Earth Surf. Process. Landf. 32, 2052–2069.

Coutinho, M.A., Tomás, P.P., 1995. Characterization of raindrop size distributions at the Vale Formoso Experimental Erosion Center. Catena 25, 187–197.

Carolina, M.A., Gabrela, C.A., Ruben, M.C., 2008. Long term variation in rainfall erosivity in Uruguay: a preliminary Fournier approach. GeoJournal 70, 257–262.

Garollina, M., Gruz, G., Mario, R., 2007. Long – term variation in rainfall erosivity in Uruguay Geography. Journal 70, 257–262.

Gilley, J.E., Finkner, S.C., 1985. Estimating soil detachment caused by raindrop impact. Trans. ASAE 28, 140–146.

Grismer, E.G., 2011. Rainfall Simulation Studies-A Review of Design, Performance and Erosion Measurement Variability. Depts. of Hydrologic Sciences and Biological & Agricultural Engineering UC Davis, California.

Grismer, M.E., Ellis, A.L., Fristensky, A., 2008. Runoff sediment particle sizes associated with soil erosion in the Lake Tahoe Basin USA. Land Degrad. Dev. 19, 331–350.

Hassan, K.F., 2011. Application of rainfall intensity–kinetic energy relationship for soil erosion prediction. Mesop. J. Agric. 39 (ISSN 815-316X).

Hudson, N., 1965. The Influence of Rainfall Mechanics on Soil Erosion. Cape Town (MSc Thesis).

Hudson, N.W., 1971. Soil Conservation. Batsford Ltd, London, p. 388.

Jayawardena, A.W., Rezaur, R.B., 2000. Measuring drop size distribution and kinetic energy of rainfall using a force transducer. Hydrol. Sci. 14, 37–49.

Kinnell, P.I.A., 1990. Modelling erosion by rain-impacted flow. Catena 17, 55–66.

Lal, R., 1998. Drop size distribution and energy load of rainstorms at Ibadan Western Nigeria. Soil Tillage Res. 48, 103–114.

Lu, J.Y., Su, C.C., Lu, T.F., Maa, M.M., 2008. Number and volume raindrop size distributions in Taiwan. Hydrol. Process. 22, 2178-2158.

Madden, L.V., Wilson, L.L., Ntahimpera, N., 1998. Calibration and evaluation of an electronic sensor for rainfall kinetic energy. Phytopathology 88, 950–959.

Marshall, J.S., Palmer, W.M., 1948. The distribution of raindrops with size. J. Meteorol. 5, 165–166.

Mclsaac, G.F., 1990. Apparent geographical and atmospheric influences on raindrop sizes and rainfall kinetic energy. J. Soil Water Conserv. 45, 663–666.

Meshesha, D.T., Tsunekawa, A., Tsubo, M., Haregeweyn, N., Adgo, E., 2013. Drop size distribution and kinetic energy load of rainfall events in the highlands of the central Rift Valley Ethiopia. Hydrol. Sci. J. http://dx.doi.org/10.1080/02626667.2013.865030.

Meshesha, D.T., Tsunekawa, A., Tsubo, M., Haregeweyn, N., Adgo, E., 2014. Evaluating spatial and temporal variations of rainfall erosivity, Case of Central Rift Valley of Ethiopia. Theor. Appl. Climatol. http://dx.doi.org/10.1007/s 00704-014-1130-2.

Morgan, R.P.C., 2005. Soil Erosion and Conversation. third edition. Blackwell Publishing, Australia.

Nyssen, J., Vandenreykena, H., Poesena, J., et al., 2005. Rainfall erosivity and variability in the Northern Ethiopian Highlands. J. Hydrol. 311, 172–187.

Oduro-Afriyie, K., 1996. Rainfall erosivity map for Ghana. Geoderma 74, 161–166.

Onaga, K., Shirai, K., Yoshinaga, A., 1988. Rainfall erosion and how to control its effect on farm land in Okinawa. In: Rimwa-nich, S. (Ed.), Land Conservation for Future Generation. Bangkok, pp. 627–639.

Pedersen, H.S., Hasholt, B., 1995. Influence of wind speed on rainsplash erosion. Catena 24, 39–54.

Renard, K.G., Freimund, J.R., 1994. Using monthly precipitation data to estimate the R-factor in the revised USLE. J. Hydrol. 15, 287–306.

Renard, K.G., Foster, G.R., Weesies, G.A., Porter, J.P., 1991. Revised universal soil loss equation. J. Soil Water Conserv. 46, 30–33.

Roose, E.J., 1975. Erosion et Ruissellement en Afrique de l'Ouest: Vingt Années de Mesures en Petites Parcelles Expérimentales. ORSTOM, Adiopodoumé, Ivory Coast.

Rosewell, C.J., 1986. Rainfall kinetic energy in eastern Australia. J. Clim. Appl. Meteorol. 25, 1695–1701.

Salles, C., Poesen, J., Sempere-Torres, D., 2002. Kinetic energy of rain and its functional relationship with intensity. J. Hydrol. 257, 256–270.

Sempere-Torres, D.S., Salles, C., Creutin, J.D., Delaffiu, G., 1992. Quantification of Soil Detachment by Raindrop Impact: Performance of Classical Formulae of Kinetic Energy in Mediterranean Storms (Proceedings of the Oslo Symposium). IAHS Publ. no. 210.

Sharma, P.P., Gupta, S.C., Foster, G.R., 1995. Raindrop-induced soil detachment and sediment transport from interrill areas. Soil Sci. Soc. Am. J. 59, 727–734.

Stocking, M.A., Elwell, H.A., 1973. Prediction of subtropical storm soil losses from field plot studies. Agric. Meteorol. 12, 193–201.

Van Dijk, A., Bruijnzeel, L., Rosewell, C., 2002. Rainfall intensity–kinetic energy relationships: a critical literature appraisal. J. Hydrol. 261, 1–23.

Wischmeier, W., Smith, D., 1958. Rainfall energy and its relationship to soil loss. Trans. AGU 39, 285–291.

Wischmeier, W., Smith, D., 1978. Predicting rainfall erosion losses. Agricultural Handbook 537. Science and Education Administration, USDA, Washington, DC.

Zanchi, C., Torri, D., 1980. Evaluation of Rainfall Energy in Central Italy. In: De Boodt, M., Gabriels, D. (Eds.), Assessment of Erosion. Wiley, London, pp. 133–142.